THE JOURNAL OF BIOLOGICAL CHEMISTRY VOL. 283, NO. 44, pp. 29920–29928, October 31, 2008

Compartmentalization of Phosphatidylinositol 4,5-Bisphosphate Signaling Evidenced Using Targeted Phosphatases*

Received for publication, July 31, 2008 Published, JBC Papers in Press, August 21, 2008, DOI 10.1074/jbc.M805921200

Corey M. Johnson[‡], Gurunadh R. Chichili[‡], and William Rodgers[‡§¶1]

From the [‡]Cardiovascular Biology Research Program, Oklahoma Medical Research Foundation, and the Departments of [§]Pathology and [¶]Microbiology and Immunology, University of Oklahoma Health Sciences Center, Oklahoma City, Oklahoma 73104

Phosphatidylinositol 4,5-bisphosphate (PIP_2) is a prevalent phosphoinositide in cell membranes, with important functions in cell signaling and activation. A large fraction of PIP_2 associates with the detergent-resistant membrane "raft" fraction, but the functional significance of this association remains controversial. To measure the properties of raft and nonraft PIP_2 in cell signaling, we targeted the PIP_2-specific phosphatase Inp54p to either the raft or nonraft membrane fraction using minimal membrane anchors. Interestingly, we observed that targeting Inp54p to the nonraft fraction resulted in an enrichment of raft-associated PIP_2 and striking changes in cell morphology, including a wortmannin-sensitive increase in cell filopodia and cell spreading. In contrast, raft-targeted Inp54p depleted the raft pool of PIP_2 and produced smooth T cells void of membrane ruffling and filopodia. Furthermore, raft-targeted Inp54p inhibited capping in T cells stimulated by cross-linking the T cell receptor, but without affecting the T cell receptor-dependent Ca^{2+} flux. Altogether, these results provide evidence of compartmentalization of PIP_2-dependent signaling in cell membranes such as predicted by the membrane raft model.

The lipid phosphatidylinositol 4,5-bisphosphate (PIP_2)[2] is important for cell growth and viability (1), exemplified by its role as the precursor for the second messengers inositol 1,4,5-triphosphate, diacylglycerol, and phosphatidylinositol 3,4,5-bisphosphate (PIP_3) (2, 3). PIP_2 is also a cofactor for activation of select membrane proteins (4); this includes proteins that function in tethering actin filaments to the plasma membrane, such as the ERM (ezrin-radixin-moesin) proteins (5) and the filamins (6). Other PIP_2-regulated membrane proteins include WASP and WAVE, which serve as effectors for the Rho GTPases in actin polymerization (7). Altogether, the properties of PIP_2 in regulating actin-associated membrane proteins underlie its important role in establishing interactions between the plasma membrane and actin cytoskeleton (8).

The diverse and important functions of PIP_2 underscore the importance of maintaining proper regulation of this lipid. As cell membranes are structurally heterogeneous (9), spatially concentrating PIP_2 in discrete domains could be one mechanism for regulating PIP_2 functions. Notably, a significant pool of the PIP_2 associates with the detergent-resistant membrane (DRM) fraction postulated to represent cholesterol-dependent membrane domains, or membrane "rafts" (10–12). As membrane rafts serve as "reaction vessels" in the plasma membrane (13), enrichment of PIP_2 in rafts may augment PIP_2-dependent pathways and production of second messengers. Alternatively, rafts may function in regulating PIP_2 signaling by sequestering it from activators in steady-state conditions, such as evidenced with certain membrane-associated kinases (14, 15).

Membrane domains such as rafts are often below the resolution of light microscopy, making direct observation of these structures difficult. Accordingly, many of the properties of the rafts have been deciphered from measurements of DRMs. One shortcoming with this approach is that the detergents used to prepare the DRMs also perturb the physical properties of the bilayer. Accordingly, it has been suggested the detergent-insoluble membranes are an artifact of sample preparation and not representative of domains in intact membranes (16, 17). Similarly, studies of rafts often utilize cholesterol-depleting agents such as methyl-β-cyclodextrin, and these compounds can cause nonspecific changes in membrane structure and function (16–19). In one example, it was shown that treating cells with methyl-β-cyclodextrin alters the membrane distribution of PIP_2 and its availability to PIP_2-binding proteins (19). However, it is not known whether this property represents a cholesterol-dependent property of PIP_2 functions or a nonspecific effect from the drug treatment.

Notably, other data show that DRMs are in fact representative of discrete membrane domains (20). For example, imaging studies measuring the plasma membrane distribution of labeled proteins and lipids show a specific clustering of DRM-associated molecules. In one recent study, using fluorescence resonance energy transfer, we showed a specific cholesterol-dependent co-clustering of reporter molecules in the plasma membrane by membrane-anchoring signals that target fluores-

* This work was supported, in whole or in part, by National Institutes of Health Grant RO1 GM070001. This work was also supported by American Heart Association Grant 0625648Z. The costs of publication of this article were defrayed in part by the payment of page charges. This article must therefore be hereby marked "*advertisement*" in accordance with 18 U.S.C. Section 1734 solely to indicate this fact.

[1] To whom correspondence should be addressed: Oklahoma Medical Research Foundation, 825 NE 13th St., MS 45, Oklahoma City, OK 73104. Tel.: 405-271-3550; Fax: 405-271-7417; E-mail: william-rodgers@omrf.org.

[2] The abbreviations used are: PIP_2, phosphatidylinositol 4,5-bisphosphate; PIP_3, phosphatidylinositol 3,4,5-trisphosphate; $DiIC_{16}$, 1,1′-dihexadecyl-3,3,3′,3′-tetramethylindocarbocyanine perchlorate; DRM, detergent-resistant membrane; GFP, green fluorescent protein; PI3K, phosphatidylinositol 3-kinase; TCR, T cell receptor; PLC, phospholipase C; PH, pleckstrin homology.

cent proteins to DRMs (21). One example was the N-terminal membrane-anchoring signal of the Src family kinase Lck. However, an alternative membrane-anchoring signal from Src, which does not target molecules to DRMs, also did not cause a cholesterol-dependent clustering of fluorescent proteins. In total, results from imaging studies show that membrane rafts are heterogeneous in nature, ranging in size from nanoclusters that are on the order of a few nanometers in size to nanodomains that have a diameter of ~50 nm and to micron-size macrodomains (22, 23). Imaging experiments have also shown colocalization of PIP_2 with raft markers in both the plasma membrane and intracellular trafficking vesicles (24–27), thus consistent with the notion that PIP_2 is enriched in rafts.

Although both membrane fractionation experiments and imaging studies show that PIP_2 is enriched in rafts, the biological significance of its raft association is poorly understood. A useful approach to measuring PIP_2 functions in cells while avoiding chemical treatments is to alter membrane PIP_2 levels using membrane-targeted PIP_2-specific phosphatases (1). One example has been targeting the catalytic domain of the yeast PIP_2-specific phosphatase Inp54p to the plasma membrane using the membrane-anchoring signal of the Src family kinase Lyn (Lyn-Inp54p) (8, 28). Expression of membrane-anchored Inp54p has demonstrated a role for PIP_2 in maintaining interactions between the plasma membrane and underlying actin cytoskeleton (8). Interestingly, the membrane-anchoring signal of Lyn, which consists of myristoylation of an N-terminal glycine and palmitoylation of an adjacent cysteine, is also an effective raft-targeting sequence (29, 30). Accordingly, the discrete phenotypes evidenced by expression of Lyn-Inp54p may reflect changes specific to the raft-associated pool of PIP_2.

Using membrane-targeting sequences from separate Src family kinases to target Inp54p to cell membranes, we observed that raft- and nonraft-targeted Inp54p caused distinct changes in the membrane pools of PIP_2 and cell phenotype. For example, enrichment of the raft pool of PIP_2 by nonraft Inp54p increased membrane ruffling and cell spreading, and depletion of this pool by raft-targeted Inp54p inhibited the ruffling as well as capping in stimulated T cells. Altogether, our findings provide evidence of sequestering of PIP_2-dependent functions between separate membrane fractions in a manner consistent with the membrane raft model but while avoiding artifacts associated with detergent treatments of cell membranes.

MATERIALS AND METHODS

Gene Construction and Expression—The Inp54p constructs each contained a minimal membrane-anchoring signal, followed by green fluorescent protein (GFP) and finally the soluble domain of Inp54p (residues 1–331) that included its active site (see Fig. 1*A*). The membrane anchors were either the first 10 amino acids of Lck (L_{10}) or the first 15 amino acids of c-Src (S_{15}) (31). The following oligonucleotides were used for amplifying the DNA sequence encoding Inp54p: 5′-ACATCAGAATTC-AACAACAACAACAACAAAACGAATTGGAAGGT (sense) and 5′-TCTAGTCTCGAGTTACGGCACTGGCGTCCCT-GTAG (antisense). The L_{10}-GFP and S_{15}-GFP coding sequences were amplified from previously described genes (31) using the following primers: 5′-ACATCAGCATCCAGAATG-GGGAGCAAGAGCAA (S_{15}, sense), 5′-ACATCACCGCGG-AGAATGGGCTGTGTCTGCAGC (L_{10}, sense), and 5′-GCTAGTAAGCTTCTTGTAACAGCTCGTCCAT (GFP, antisense). The underlined nucleotides identify the restriction sites for EcoRI, XhoI, BamHI, SacII, and HindIII, respectively, which were used for directional cloning in pLenti (Invitrogen). The genes were subcloned into pLenti and oriented for control of expression by a 5′-long terminal repeat.

Cell Cultures and Transfections—Jurkat T cells (clone E6-1) were cultured in RPMI 1640 medium with 10% fetal bovine serum and supplemented with L-glutamine and antibiotics. 293T cells were grown in Dulbecco's modified Eagle's medium with 10% fetal bovine serum and supplemented with antibiotics. All cells were maintained at 37 °C in the presence of 5% CO_2.

For gene expression, 293T cells were transfected by $CaPO_4$ (Invitrogen) using 10 μg of plasmid DNA for a 50% confluent 6-cm plate. Jurkat cells were transfected by electroporation as described (32). Following transfection, Jurkat cells were cultured in AIM V medium (Invitrogen) for 48 h and then harvested for experimentation.

Membrane Fractionation—Approximately 10^7 cells were lysed by incubation at 4 °C for 20–30 min with 750 μl of 1% Triton X-100. Next, the samples were homogenized in a Dounce homogenizer (eight strokes) and centrifuged for 5 min at 4000 rpm (Eppendorf Model 5417C, Brinkmann Instruments). The supernatant was collected, and the raft and nonraft membrane fractions were separated by equilibrium centrifugation using a discontinuous sucrose gradient (14). Following centrifugation, the gradients were fractionated from the top.

PIP_2 Measurement—Phosphoinositide extraction was performed as described (33) with minor adjustments. In brief, 3 ml of ice-cold chloroform/methanol/HCl (2:4:0.1) was added to the pooled gradient fractions corresponding to the raft (gradient fractions 2–4) (see Fig. 1 in Ref. 21) and nonraft (gradient fractions 7–10) (see Fig. 1 in Ref. 21) membrane fractions. The samples were mixed vigorously for 30 s and then incubated on ice for 15 min. To induce a phase separation, 1 ml of ice-cold chloroform was added with 1 ml of 1.76% KCl, 100 mM citric acid, 100 mM Na_2HPO_4, 5 mM EDTA, and 5 mM tetrabutylammonium hydrogen sulfate. Samples were mixed for 30 s and incubated on ice for 5 min. Samples were then centrifuged for 10 min at 2000 × *g*.

After centrifugation, the organic phase (bottom) was collected, dried, and resuspended in a minimal volume (~10 μl) of solvent (4:3:1 chloroform/methanol/water). Samples were spotted onto nitrocellulose membrane using a Bio-Rad dot blot vacuum manifold. PIP_2 was detected by immunoblotting using a monoclonal antibody (Echelon Biosciences Inc., Salt Lake City, UT) at a final concentration of 1 μg/ml, followed by a biotinylated secondary antibody. The final step was horseradish peroxidase conjugated to streptavidin (Vector Laboratories, Burlingame, CA). The membrane was developed using enhanced chemiluminescence (GE Healthcare, Buckinghamshire, UK) and detected with a Lumi-Imager F1 workstation (Roche Applied Science, Mannheim, Germany).

Cell Labeling and Imaging—Imaging was performed using either a Zeiss LSM510 microscope or a Zeiss Axioplan 2i

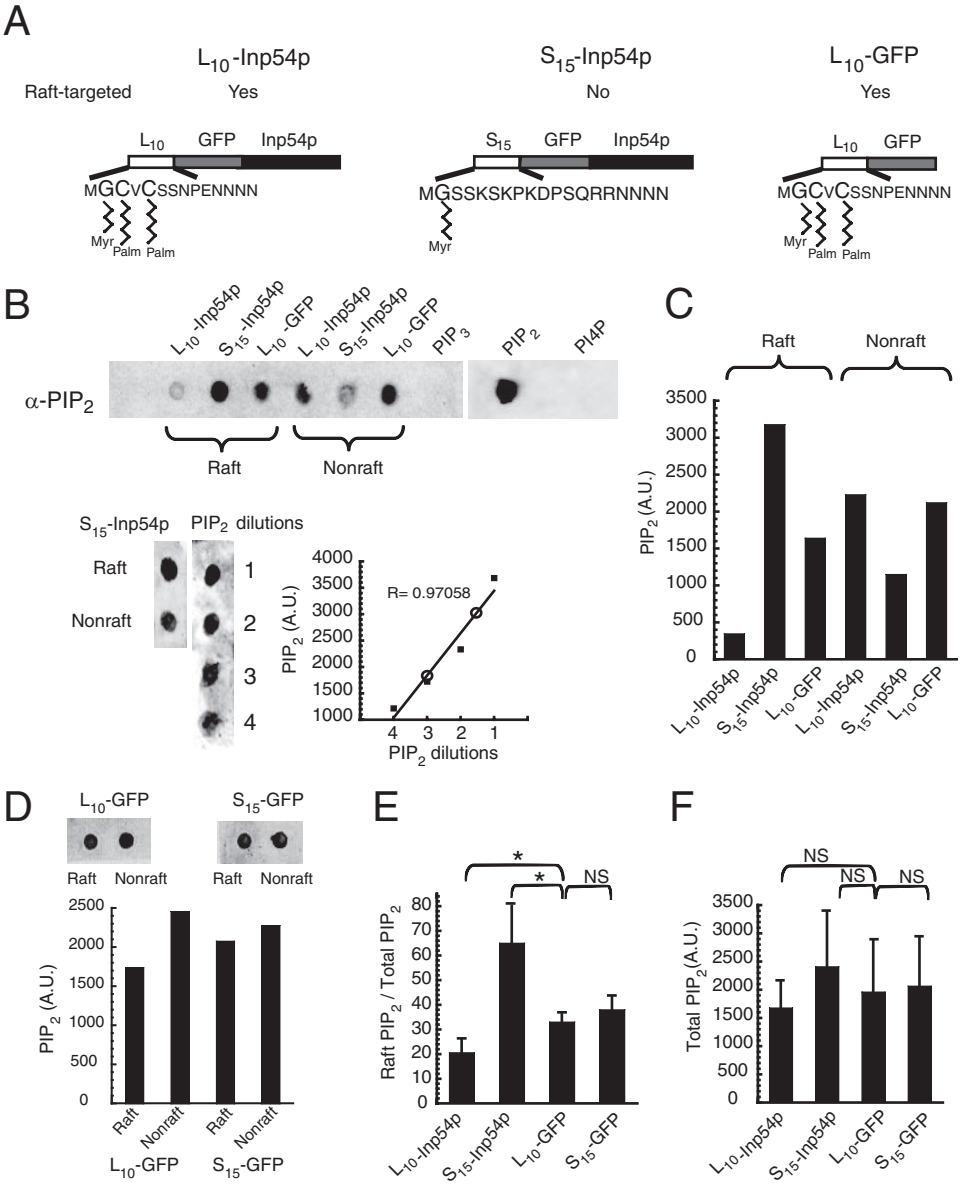

FIGURE 1. **Membrane-targeted Inp54p molecules cause distinct changes in raft and nonraft PIP$_2$.** *A*, targeting of the PIP$_2$-specific phosphatase Inp54p to raft and nonraft membrane fractions. The constructs contained either the first 10 amino acids of Lck (L_{10}) or the first 15 amino acids of c-Src (S_{15}) for membrane association, followed by GFP and finally the soluble domain of Inp54p (L_{10}-Inp54p and S_{15}-Inp54p, respectively). L_{10} targets proteins to the detergent-resistant raft fraction, and S_{15} restricts proteins to the detergent-soluble nonraft fraction (21). *Myr* and *Palm* indicate sites of myristoylation and palmitoylation, respectively, of the indicated residues in the membrane-anchoring signals. A third construct consisting of membrane-anchored GFP (L_{10}-GFP) was used as a control. *B*, measurement of changes in membrane PIP$_2$ pools by L_{10}-Inp54p and S_{15}-Inp54p (*upper panel*). 293T cells expressing either L_{10}-Inp54p or S_{15}-Inp54p were lysed with Triton X-100, and the raft and nonraft membrane fractions were separated by sucrose gradient equilibrium centrifugation. Following separation, the gradient fractions containing the respective membrane fractions were pooled and extracted, and PIP$_2$ was measured in each by immunoblotting. PIP$_3$, PIP$_2$, and phosphatidylinositol 4-phosphate (*PI4P*) represent purified lipids that were measured in parallel as controls for antibody specificity. Immunoblotting a range of the PIP$_2$ standards together with a set of samples from cells that expressed S_{15}-Inp54p showed that PIP$_2$ extracted from cells was within the dynamic range of the measure (*lower panel*). In the accompanying plot, values for the S_{15}-Inp54p raft and nonraft fractions are represented by *open circles*. *A.U.* denotes arbitrary units. *C*, quantitation of the immunoblot in *B*. *D*, measurement of membrane PIP$_2$ pools for cells expressing L_{10}-GFP and S_{15}-GFP as a control for any sequestering of PIP$_2$ by the S_{15} sequence. Quantitation of the dots is shown in the graph below. *E*, average of measurements from three separate trials. These results are represented as the fraction of total PIP$_2$ that was raft-associated. *F*, total lipids measured for PIP$_2$. In *E* and *F*, the *error bars* represent S.E. *, $p \leq 0.05$ by Student's *t* test; *NS* (not significant), $p > 0.38$.

upright fluorescence microscope (Oklahoma Medical Research Foundation Cell Imaging Core Facility). The images were collected using a 100× oil objective (1.4 numerical aperture). Three-dimensional projection images were generated from confocal stacks that were collected by optically sectioning along the *z* axis at an interval of 0.24 μm. Before three-dimensional reconstruction, the confocal stacks were deconvolved using AutoDeblur (AutoQuant Imaging, Inc., Watervliet, NY). The projection images were produced using iVision (BioVision Technologies, Exton, PA). All other image processing and quantitation were performed using iVision.

For imaging of T cell capping, cells were stimulated using OKT3-coated polystyrene beads as described (34). Following stimulation, the samples were fixed using 2% paraformaldehyde and then permeabilized with 0.2% Triton X-100 in phosphate-buffered saline. F-actin was labeled by incubation with 0.1 μg/ml Texas Red-labeled phalloidin (Invitrogen) for 30–45 min at 37 °C. Capping was quantitated by dividing the average fluorescence intensity of the plasma membrane in contact with the OKT3-coated bead by the average fluorescence intensity of the remaining plasma membrane. Cells were scored positive for capping if the ratio was 1.5 or greater. Histograms of relative fluorescence enrichment in the caps were prepared using IGOR Pro software (WaveMetrics, Inc., Lake Oswego, OR).

Ca^{2+} Flux Measurements—For detection of Ca^{2+} during stimulation, Jurkat T cells were labeled by incubation for 30 min in 2 μM Indo-1 (Invitrogen) at 37 °C. Following labeling, the cells were suspended in 15 mM HEPES (pH 7.4) supplemented with 140 mM NaCl, 5 mM KCl, 1 mM $MgCl_2$, 1.8 mM $CaCl_2$, and 10 mM glucose. The Ca^{2+} flux was measured by flow cytometry (MOFLO, DakoCytomation, Fort Collins, CO) based on the change in the fluorescence emission at 475 and 400 nm. Excitation for Indo-1 was at 390 nm. To limit the measurements to transfected cells, the samples were gated on those expressing GFP. GFP was detected using 488 nm excitation with a green band-pass filter centered at 530 nm for emission. The temperature of the instrument was maintained

at 37 °C, and the flow rate was maintained by a base sheath pressure of 60 ± 1 p.s.i. A base line was achieved by passing the cells for ~1 min prior to addition of OKT3. After the OKT3-dependent flux was complete, ionomycin was added to determine the maximal flux capacity of the cells. Store-operated channel Ca^{2+} flux was measured in the same manner as the total flux, except the buffer contained 0.05 μM EGTA rather than $CaCl_2$. Following the initial flux from release of intracellular stores, Ca^{2+} (1 mM stock) was added back to the sample to a final concentration of 10 mM.

RESULTS

Membrane Raft- and Nonraft-targeted Inp54p Molecules Cause Distinct Changes in PIP_2 Membrane Pools—The membrane-targeted Inp54p molecules used in this study are illustrated in Fig. 1*A*. Specifically, we targeted Inp54p to cell membranes using either the N-terminal 10 residues of Lck (L_{10}) or the N-terminal 15 residues of Src (S_{15}). We have described the L_{10} and S_{15} membrane-anchoring signals previously (31) and showed that the L_{10} sequence efficiently targets peptides to the DRM raft fraction and that the S_{15} sequence limits peptides to the detergent-soluble nonraft fraction. As a control to identify changes in the PIP_2 pools and cell phenotype that were specific to the phosphatase activity, we expressed a third construct containing the L_{10} anchor and GFP but no Inp54p (L_{10}-GFP).

To determine the effect of the targeted Inp54p molecules on the raft and nonraft pools of PIP_2, we measured the PIP_2 present in each membrane fraction after expressing L_{10}-Inp54p, S_{15}-Inp54p, or L_{10}-GFP. For this experiment, we extracted the lipids of the raft and nonraft fractions following separation of the membrane fractions by sucrose gradient equilibrium centrifugation (see "Materials and Methods"). In Fig. 1*B* is an immunoblot measuring the PIP_2 present in each membrane fraction of transfected cells, and in Fig. 1*C* are the results from quantitating the blot. These data show that expression of L_{10}-Inp54p decreased the raft-associated pool of PIP_2, whereas S_{15}-Inp54p both increased the amount of raft PIP_2 and decreased the PIP_2 in the nonraft fraction. Furthermore, the changes in raft and nonraft PIP_2 by S_{15}-Inp54p were specific to the Inp54p domain because expression of a GFP molecule containing the S_{15} anchor alone (S_{15}-GFP) demonstrated similar levels of PIP_2 in each fraction as L_{10}-GFP (Fig. 1, *D* and *E*). By averaging the results from several trials, we determined that L_{10}-Inp54p decreased by 10% the fraction of total PIP_2 that was raft-associated, whereas S_{15}-Inp54p increased this ratio by 2-fold (Fig. 1*E*). Notably, neither Inp54p construct caused a statistically significant change in the total PIP_2 levels of the cells (Fig. 1*F*).

T Cells Demonstrate Distinct Morphologies and Cell Spreading Based on Targeted Inp54p Expression—In T cells, PIP_2 and its effectors are necessary for cell activation (35–37). To determine whether raft and nonraft pools of PIP_2 in T cells are functionally distinct, we measured Jurkat T cells expressing L_{10}-Inp54p, S_{15}-Inp54p, or control L_{10}-GFP. Interestingly, we observed distinct morphologies from expression of the separate Inp54p molecules (Fig. 2*A*). For example, T cells that expressed raft-targeted L_{10}-Inp54p (Fig. 2*A*, *left panel*) often exhibited a smooth morphology that was void of the membrane ruffles and filopodia that occurred in control cells that expressed L_{10}-GFP

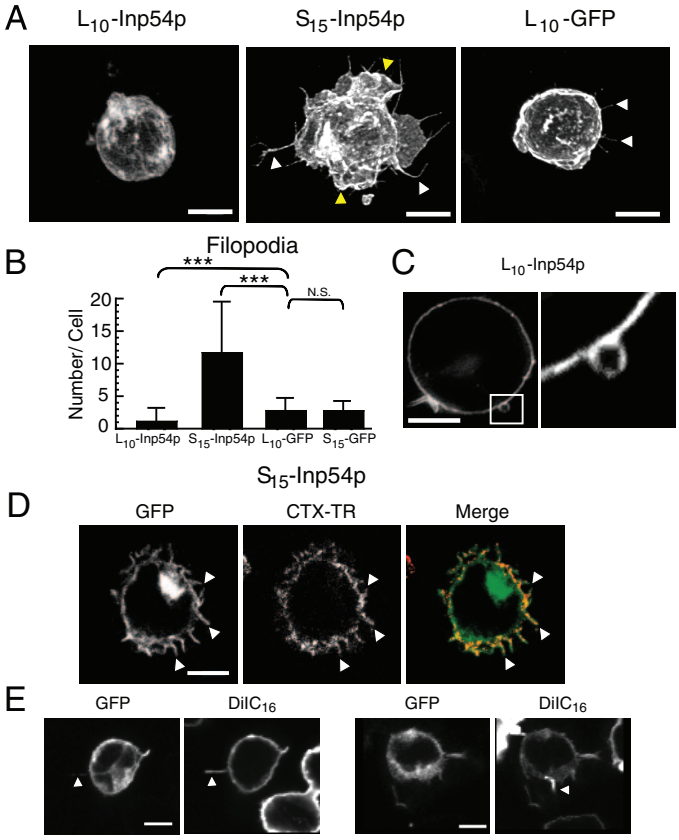

FIGURE 2. **Cell morphologies from expression of the membrane-targeted Inp54p molecules.** *A*, projection images of Jurkat T cells that expressed L_{10}-Inp54p, S_{15}-Inp54p, or L_{10}-GFP. The images were acquired using confocal microscopy and detected using GFP fluorescence. The *white* and *yellow arrowheads* indicate filopodia and membrane ruffling, respectively. *B*, quantitation of filopodia in transfected T cells. Filopodia in cells that expressed L_{10}-Inp54p, S_{15}-Inp54p, L_{10}-GFP, or S_{15}-GFP were counted using wide-field microscopy. The graph represents the average of 90 cells measured in three independent trials. The *error bars* represent S.E. ***, $p \leq 0.005$ by Student's *t* test; *N.S.*, not significant. *C*, representative example of the membrane blebs observed in cells that expressed L_{10}-Inp54p. The *right panel* is a higher magnification of the region indicated by the *square* in the *left panel*. *D*, confocal images of a T cell double-labeled with S_{15}-Inp54p and cholera toxin conjugated to Texas Red (*CTX-TR*). The *arrowheads* indicate examples of double-labeled filopodia. *E*, confocal images of Jurkat cells double-labeled with S_{15}-Inp54p and $DiIC_{16}$. The *arrowheads* indicate filopodia labeled with $DiIC_{16}$ but not S_{15}-Inp54p. *Scale bars* = 5 μm.

(*right panel*). We also observed membrane blebs in the L_{10}-Inp54p samples (Fig. 2*C*), similar to those described for cells expressing Lyn-Inp54p (8). The blebs represent regions of the plasma membrane that bubble outward and can be due to poor association of the membrane with the underlying actin cytoskeleton (38).

In contrast to L_{10}-Inp54p, T cells that expressed S_{15}-Inp54p exhibited a striking morphology that contained numerous filopodia and extensive membrane folding compared with that of the control samples (Fig. 2*A*, *middle panel*). We quantitated the effects of each Inp54p construct on cell morphology by counting the number of filopodia in T cells expressing either L_{10}-Inp54p or S_{15}-Inp54p. As controls, we expressed either L_{10}-GFP or S_{15}-GFP. These measurements showed an increase in filopodial number upon S_{15}-Inp54p expression, whereas L_{10}-Inp54p caused a decrease in filopodial number relative to the control samples (Fig. 2*B*).

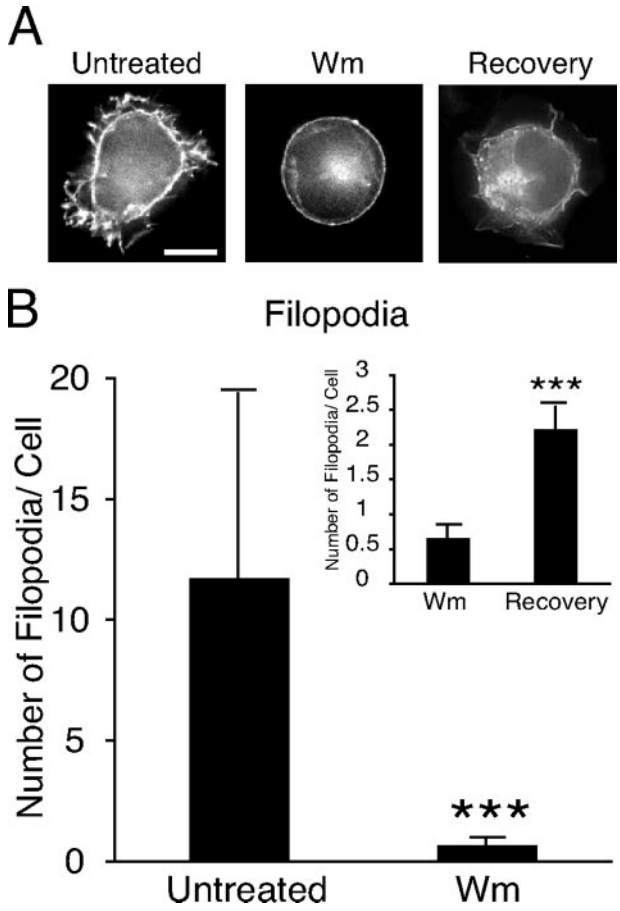

FIGURE 3. **S_{15}-Inp54p-dependent filopodial growth is PI3K-dependent.** *A*, representative images of T cells expressing S_{15}-Inp54p that were treated with wortmannin (*Wm*) or treated with wortmannin, washed, and allowed to recover in growth media for 2 h (*Recovery*). *Scale bar* = 5 μm. *B*, quantitation of the number of filopodia in each set of conditions. The data represent the average of 90 cells measured in three separate trials. ***, $p \leq 0.005$ by Student's *t* test.

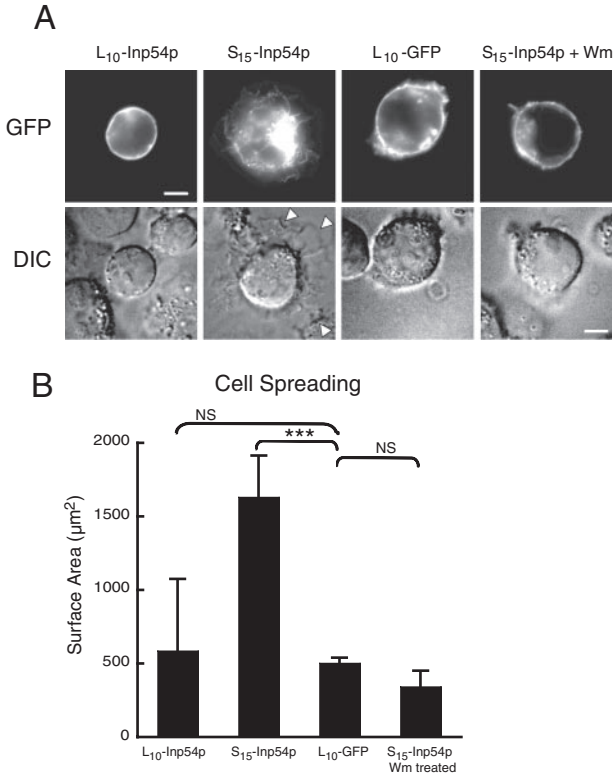

FIGURE 4. **T cells expressing S_{15}-Inp54p exhibit increased cell spreading in a PI3K-dependent manner.** *A*, confocal (*upper panels*) and differential interference contrast (*DIC*; *lower panels*) images of T cells expressing L_{10}-Inp54p, S_{15}-Inp54p, or L_{10}-GFP. One set of cells expressing S_{15}-Inp54p was treated with wortmannin (*Wm*) before fixation. The *arrowheads* in the S_{15}-Inp54p sample indicate the edges of cell spreading. *Scale bars* = 5 μm. *B*, averaged results measuring the surface area of transfected Jurkat T cells seeded onto poly-L-lysine-coated coverslips. The data are from 60 cells measured in three independent trials using differential interference contrast imaging. ***, $p \leq 0.005$ by Student's *t* test; *NS* (not significant), $p > 0.05$.

The increase in cell filopodia upon S_{15}-Inp54p expression coincided with an increase in raft-associated PIP_2 (Fig. 1), suggesting that the filopodia may contain raft-enriched membrane. To test this hypothesis, we stained T cells expressing S_{15}-Inp54p with biotinylated cholera toxin B subunit and secondary streptavidin conjugated to Texas Red. In Fig. 2*D* is an example showing labeling of filopodia by Texas Red-conjugated cholera toxin. Interestingly, we often noted that Texas Red-conjugated cholera toxin appeared as puncta localized along the processes, suggestive of rafts localized on the filopodia. We also detected staining of the filopodia with the raft marker $DiIC_{16}$ (Fig. 2*E*), although in this case, the labeling was not enriched in puncta. Furthermore, in some cases, we observed efficient labeling of filopodia by $DiIC_{16}$ that were barely detectable with the S_{15}-Inp54p label (Fig. 2*E*, *white arrowheads*). This finding is again suggestive of enrichment of raft membranes in the cell processes. We conclude from these data that the filopodia in cells that expressed S_{15}-Inp54p contained membrane rafts, and this may reflect enrichment of PIP_2 in membrane rafts upon S_{15}-Inp54p expression.

S_{15}-Inp54p-dependent Changes in Cell Morphology Are Phosphatidylinositol 3-Kinase (PI3K)-dependent—An important effector of PIP_2 signaling in membrane-actin interactions is the PI3K product PIP_3 (3). To determine whether the T cell morphology upon S_{15}-Inp54p expression was PIP_3-dependent, we measured cells expressing S_{15}-Inp54p and treated with wortmannin. Cell imaging showed that wortmannin inhibited the membrane ruffling and filopodia that occurred in the untreated cells (Fig. 3*A*), and quantitation showed that wortmannin reduced the average number of filopodia by 10-fold (Fig. 3*B*). We also observed that washing away the wortmannin following drug treatment resulted in a return of the membrane ruffling and filopodia 2 h later (Fig. 3*A*, *right panel*), albeit not to the number measured in untreated cells (Fig. 3*B*). We interpret these data as evidence that the cell morphologies that occurred upon S_{15}-Inp54p expression were PI3K-dependent.

Altered Cell Spreading by Targeted Inp54p Expression—Cell spreading occurs by activation of surface adhesion molecules, many of which are PIP_2-dependent (39). Similarly, we observed in T cells expressing S_{15}-Inp54p an increase in cell spreading on poly-L-lysine, often represented by an extension of a thin sheet of membrane from the cell body (Fig. 4*A*, *arrowheads*). We quantitated the cell spreading by measuring the area of the cell where it contacted the substratum, and this showed that S_{15}-Inp54p caused a 2–3-fold increase in the cell area over that of cells expressing either L_{10}-GFP or L_{10}-Inp54p. Furthermore, wortmannin inhibited the S_{15}-Inp54p-dependent spreading

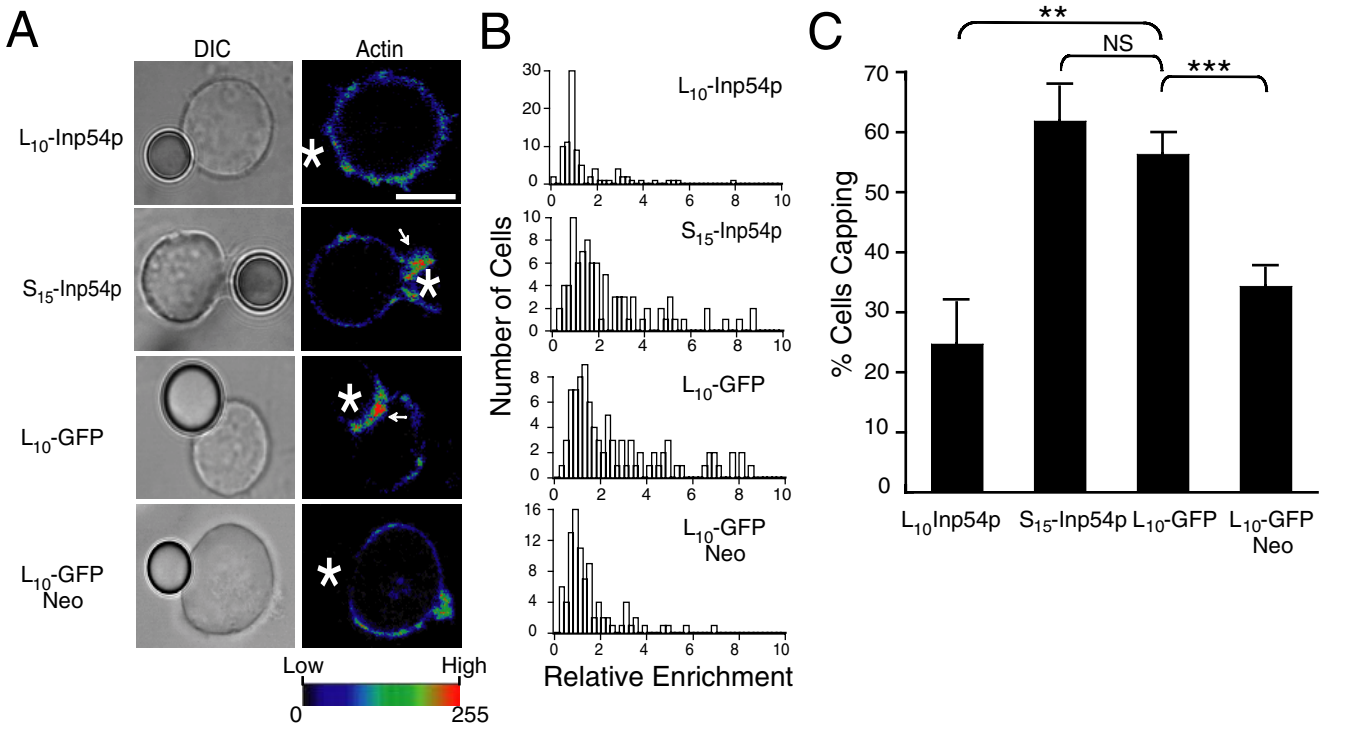

FIGURE 5. **L_{10}-Inp54p inhibits actin capping in stimulated T cells.** *A*, differential interference contrast (*DIC*) and confocal images of stimulated Jurkat T cells expressing L_{10}-Inp54p, S_{15}-Inp54p, L_{10}-GFP, or L_{10}-GFP treated with neomycin (*Neo*). Following stimulation, the samples were stained with Texas Red-conjugated phalloidin to detect F-actin. The fluorescence intensities are represented by pseudocolor, and the color assignment for intensity values is shown at the bottom. The *asterisks* indicate the positions of the antibody-coated beads. The *arrows* indicate actin-enriched membrane caps at the cell-bead interface. *B*, histograms of the relative enrichment of F-actin at the bead-cell interface measured in ~100 bead-cell conjugates. *C*, quantitation of the frequency of F-actin capping of each sample measured using confocal microscopy. A cell was scored as positive for capping when the mean fluorescence intensity of the bead-cell interface divided by the mean fluorescence intensity of the rest of the cell was 1.5 or greater. Percent cells positive for capping for each sample is graphed. The results were averaged from 90 separate bead-cell conjugates measured in three separate trials. **, $p \leq 0.01$ by Student's *t* test; ***, $p \leq 0.005$; *NS* (not significant), $p > 0.05$.

(Fig. 4, *A* and *B*). Thus, the increased spreading from S_{15}-Inp54p expression was also a PI3K-dependent property.

Raft-targeted Inp54p Inhibits T Cell Capping following Stimulation—T cells stimulated by cross-linking the T cell receptor (TCR) generate actin-rich membrane caps at the site of receptor cross-linking (40). To determine the effect of the membrane-targeted Inp54p molecules on membrane capping, transfected T cells were stimulated using 6-μm polystyrene beads coated with an antibody specific to human CD3 (OKT3). To detect the capping, samples were fixed and stained with Texas Red-conjugated phalloidin and measured by confocal microscopy.

In Fig. 5*A* are representative images of bead-cell conjugates that show an inhibition of capping by L_{10}-Inp54p expression. For example, the cells that expressed either S_{15}-Inp54p or control L_{10}-GFP exhibited a 2–3-fold enrichment of F-actin at the bead-cell interface, but the cells that expressed L_{10}-Inp54p demonstrated no such capping. Furthermore, pretreating cells expressing L_{10}-GFP with neomycin to sequester PIP_2 (41) also inhibited the T cell capping, and this is consistent with the inhibition by L_{10}-Inp54p occurring upon phosphatase-dependent changes in the PIP_2 pools. The inhibition of T cell capping by L_{10}-Inp54p and neomycin is also represented by the histograms in Fig. 5*B*, which represents data from measuring the relative fluorescence enrichment at the bead-cell interface of ~100 conjugates. Finally, in a separate analysis, cells were scored as capped if the average intensity at the bead-cell interface was 50% or greater than the remaining membrane. The fraction of cell-bead conjugates in each sample that exhibited capping under this criterion is plotted in Fig. 5*C*, and these data show that the inhibition by L_{10}-Inp54p was both specific and statistically significant.

PIP_2 is important for a TCR-dependent Ca^{2+} flux that drives remodeling of the cell cytoskeleton and associated membrane (35). Accordingly, one interpretation of the results in Fig. 5 is that the reduced actin capping by L_{10}-Inp54p and neomycin is due to an inhibition of the TCR-dependent Ca^{2+} flux. However, in contrast to the capping, we observed that neither L_{10}-Inp54p nor S_{15}-Inp54p significantly affected the total Ca^{2+} flux relative to control cells (Fig. 6, *A* and *B*). Furthermore, the add-back assays in Fig. 6 (*C* and *D*) show that the Inp54p constructs also did not affect the release of either intracellular Ca^{2+} stores or store-operated channels. We therefore conclude that the inhibition of capping by L_{10}-Inp54p did not occur by blocking Ca^{2+} signals downstream of the TCR.

DISCUSSION

Membrane fractionation experiments show that a significant pool of cellular PIP_2 associates with the cholesterol-dependent membrane rafts (10, 11). However, the functional significance of PIP_2 compartmentalization has been unclear and even controversial. In this study, we used separate targeted forms of the PIP_2-specific phosphatase Inp54p to measure the properties of

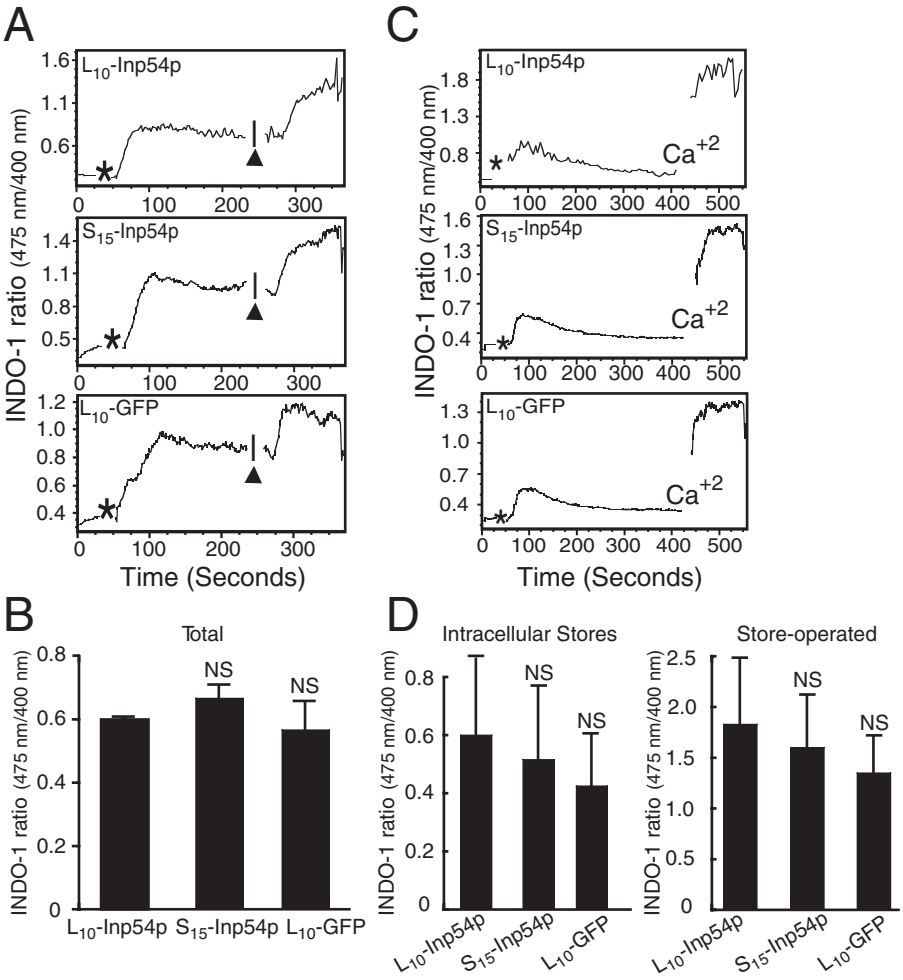

FIGURE 6. **Ca^{2+} flux in stimulated T cells is not altered by membrane-targeted Inp54p expression.** *A*, intracellular Ca^{2+} flux following TCR stimulation of Jurkat T cells expressing L_{10}-Inp54p, S_{15}-Inp54p, or L_{10}-GFP. T cells labeled with Indo-1 were measured by flow cytometry and stimulated with OKT3 antibody (asterisks). Ionomycin addition is indicated by the black arrowheads. *B*, The total intracellular Ca^{2+} flux averaged from three independent trials. *C*, The store-operated Ca^{2+} flux was measured the same as (*A*), but cells were measured in buffer containing 0.05 μM EGTA to discriminate between flux from intracellular stores and flux from store-operated channels. Ca^{2+} indicates the time point when Ca^{2+} was added. *D*, The Ca^{2+} flux from store-operated channels averaged from three separate trials. In *B* and (*D*), NS, $p > 0.05$ by Student's *t* test.

PIP_2 in raft and nonraft fractions. Specifically, Inp54p was either targeted to the raft fraction using the membrane anchor of the Src family kinase Lck or restricted to the nonraft fraction using the membrane anchor of Src. Consistent with the membrane raft model, our data show phenotypes that correspond to specific changes in the raft-associated pool of PIP_2. For example, expression of S_{15}-Inp54p increased the fraction of PIP_2 in the raft fraction, and this coincided with increased membrane ruffling, cell spreading, and growth of surface filopodia. Conversely, L_{10}-Inp54p caused a decrease in raft-associated PIP_2, and this coincided with cells that were smooth in appearance and void of membrane ruffles and filopodia as well as inhibited in their TCR-dependent capping.

Neither Inp54p molecule significantly changed the amount of total PIP_2, further indicating that the phenotypes reported here were due to changes in discrete pools of PIP_2 rather than its global levels in the membrane. In the case of S_{15}-Inp54p, the enrichment of raft PIP_2 was offset by a decrease in nonraft PIP_2. However, no such offset that accommodated a decrease in raft PIP_2 by L_{10}-Inp54p expression was observed. One explanation for this discrepancy is that L_{10}-Inp54p decreased the total PIP_2, but below a level that was detectable by our method.

One possible mechanism for the enrichment of PIP_2 in rafts by S_{15}-Inp54p is an increase in the expression of protein factors such as MARCKS (myristoylated alanine-rich C kinase substrate) and GAP-43. These proteins bind PIP_2 and cause its partitioning into raft-like liquid-ordered phase lipids (49, 50). Alternatively, depletion of nonraft PIP_2 may activate synthesis of PIP_2 specifically in the membrane rafts. Overall, the similar level of total PIP_2 in cells expressing the targeted phosphatases shows a coupling of PIP_2 synthesis with its consumption by Inp54p. PIP_2 levels in cell membranes in general undergo extensive regulation, underscored by the quick re-establishment of steady-state levels following its hydrolysis by phospholipase C (PLC) during cell activation (51). Substantial reductions of PIP_2 by drug treatment have global effects on plasma membrane structure (19), and this reflects the multiplicity of functions of PIP_2 in establishing and maintaining membrane architecture. Our data show that at least some of the functions of PIP_2 are regulated by its compartmentalization between raft and nonraft membrane fractions.

Interestingly, the membrane ruffling and cell spreading brought about by S_{15}-Inp54p were sensitive to wortmannin, showing that these changes occur through a PIP_3-dependent mechanism. This could occur through basal PI3K activity acting on the elevated raft-associated PIP_2, thereby elevating the PIP_3 content of the membrane and activating PIP_3-dependent enzymes. Jurkat cells lack expression of the PIP_3-specific phosphatase PTEN, and this will allow for an accumulation of PIP_3 (42). However, the S_{15}-Inp54p-dependent morphology was not restricted to Jurkat cells because we also observed extensive membrane ruffling and filopodia in HeLa cells transfected with this construct (data not shown). Interestingly, expression of dominant-negative and constitutively active forms of the GTPase Rac in Jurkat cells generates cell morphologies similar to those we report here for L_{10}-Inp54p and S_{15}-Inp54p, respectively (43). Rac is a downstream effector of the guanine nucleotide exchange factor Vav (44), which itself is a PIP_3-dependent enzyme. Accordingly, the changes in cell phenotype that we evidenced with the mem-

brane-targeted Inp54p molecules may reflect signaling in the Vav-Rac pathway affected by the altered levels of raft PIP_2.

In stimulated T cells, PLCγ1 is recruited to the plasma membrane through binding to LAT (linker of activated T cells) (45, 46). Membrane recruitment of PLCγ1 is followed by production of inositol 1,4,5-trisphosphate through hydrolysis of PIP_2, which then serves as a second messenger to initiate the TCR-dependent Ca^{2+} flux. LAT is constitutively associated with membrane rafts (47), suggesting that much of the PLCγ1 is proximal to raft pools of PIP_2. However, our data show that reducing these pools using L_{10}-Inp54p did not significantly affect the Ca^{2+} flux. One interpretation of this finding is that PLCγ1 utilizes nonraft PIP_2 more than predicted based on the proximity of LAT to raft PIP_2. Utilization of nonraft PIP_2 by LAT-associated PLCγ1 may also account for the ability of a nonraft form of LAT to fully restore the TCR-dependent Ca^{2+} flux when expressed in LAT-deficient thymocytes (48). Altogether, these findings illustrate the caution that should be exercised in interpreting membrane fractionation data as well as the complexities relating to regulation and activation of PIP_2-dependent signaling.

In contrast to the notion of membrane domains enriched with PIP_2, one recent study using the pleckstrin homology (PH) domain of PLCδ1 to detect PIP_2 did not observe clustering of the lipid in the plasma membrane (51). PH domains are a useful tool in qualitative measurements of phosphoinositides, such as detecting their turnover during cell signaling (52, 53). However, their utility in quantitative measurements is less certain. For example, the level of detection of the lipids by the probes is likely proportional to their level of expression, which itself will vary from cell to cell in an individual trial and between separate trials in each experiment. Furthermore, PH domains are often nonspecific in nature because many bind efficiently to more than one phosphoinositide species or their metabolites (54). For example, the PH domain from PLCδ1 binds both PIP_2 and the PLC product inositol 1,4,5-trisphosphate (55). Accordingly, additional experiments using more quantitative probes may demonstrate properties for the PIP_2 membrane distribution that are more consistent with its enrichment in membrane rafts.

Altogether, the factors that affect protein and lipid distributions in cell membranes remain an ongoing topic of studies of membrane structure. The membrane localization of PIP_2 is a particularly important question because of its pivotal role in many membrane functions and cell signaling events. Membrane fractionation experiments show that a significant fraction of PIP_2 occurs in membrane rafts. We provide evidence here showing that this represents a compartmentalization of PIP_2 functions in T cells, where raft-associated PIP_2 corresponds to a discrete pool of molecules that confer distinct phenotypes on T cells when modified using targeted PIP_2-specific phosphatases. Further experiments are, however, necessary to better define the character of raft-associated PIP_2 in biological membranes and the mechanism for PIP_2 enrichment in these structures.

Acknowledgments—We thank Jacob Bass (Oklahoma Medical Research Foundation Flow Cytometry Core Facility) for flow cytometry assistance, L. Tsiokas for helpful discussions, and K. Moore and M. Coggeshall for comments on the manuscript.

REFERENCES

1. Di Paolo, G., and De Camilli, P. (2006) *Nature* **443,** 651–657
2. Majerus, P. W., Connolly, T. M., Deckmyn, H., Ross, T. S., Bross, T. E., Ishii, H., Bansal, V. S., and Wilson, D. B. (1986) *Science* **234,** 1519–1526
3. Rameh, L. E., and Cantley, L. C. (1999) *J. Biol. Chem.* **274,** 8347–8350
4. McLaughlin, S., Wang, J., Gambhir, A., and Murray, D. (2002) *Annu. Rev. Biophys. Biomol. Struct.* **31,** 151–175
5. Ilani, T., Khanna, C., Zhou, M., Veenstra, T. D., and Bretscher, A. (2007) *J. Cell Biol.* **179,** 733–746
6. Stossel, T. P., Condeelis, J., Cooley, L., Hartwig, J. H., Noegel, A., Schleicher, M., and Shapiro, S. S. (2001) *Nat. Rev. Mol. Cell Biol.* **2,** 138–145
7. Takenawa, T., and Suetsugu, S. (2007) *Nat. Rev. Mol. Cell Biol.* **8,** 37–48
8. Raucher, D., Stauffer, T., Chen, W., Shen, K., Guo, S., York, J. D., Sheetz, M. P., and Meyer, T. (2000) *Cell* **100,** 221–228
9. Engelman, D. M. (2005) *Nature* **438,** 578–580
10. Pike, L. J., and Casey, L. (1996) *J. Biol. Chem.* **271,** 26453–26456
11. Pike, L. J., and Miller, J. M. (1998) *J. Biol. Chem.* **273,** 22298–22304
12. Laux, T., Fukami, K., Thelen, M., Golub, T., Frey, D., and Caroni, P. (2000) *J. Cell Biol.* **149,** 1455–1472
13. Tian, T., Harding, A., Inder, K., Plowman, S., Parton, R. G., and Hancock, J. F. (2007) *Nat. Cell Biol.* **9,** 905–914
14. Rodgers, W., and Rose, J. K. (1996) *J. Cell Biol.* **135,** 1515–1523
15. Young, R. M., Zheng, X., Holowka, D., and Baird, B. (2005) *J. Biol. Chem.* **280,** 1230–1235
16. Heerklotz, H. (2002) *Biophys. J.* **83,** 2693–2701
17. Heerklotz, H., Szadkowska, H., Anderson, T., and Seelig, J. (2003) *J. Mol. Biol.* **329,** 793–799
18. Pizzo, P., Giurisato, E., Tassi, M., Benedetti, A., Pozzan, T., and Viola, A. (2002) *Eur. J. Immunol.* **32,** 3082–3091
19. Kwik, J., Boyle, S., Fooksman, D., Margolis, L., Sheetz, M. P., and Edidin, M. (2003) *Proc. Natl. Acad. Sci. U. S. A.* **100,** 13964–13969
20. Hancock, J. F. (2006) *Nat. Rev. Mol. Cell Biol.* **7,** 456–462
21. Chichili, G. R., and Rodgers, W. (2007) *J. Biol. Chem.* **282,** 36682–36691
22. Rodgers, W., Farris, D., and Mishra, S. (2005) *Trends Immunol.* **26,** 97–103
23. Jacobson, K., Mouritsen, O. G., and Anderson, R. G. (2007) *Nat. Cell Biol.* **9,** 7–14
24. Parmryd, I., Adler, J., Patel, R., and Magee, A. I. (2003) *Exp. Cell Res.* **285,** 27–38
25. Huang, S., Lifshitz, L., Patki-Kamath, V., Tuft, R., Fogarty, K., and Czech, M. P. (2004) *Mol. Cell. Biol.* **24,** 9102–9123
26. Golub, T., and Caroni, P. (2005) *J. Cell Biol.* **169,** 151–165
27. Rozelle, A. L., Machesky, L. M., Yamamoto, M., Driessens, M. H., Insall, R. H., Roth, M. G., Luby-Phelps, K., Marriott, G., Hall, A., and Yin, H. L. (2000) *Curr. Biol.* **10,** 311–320
28. Wiradjaja, F., Ooms, L. M., Whisstock, J. C., McColl, B., Helfenbaum, L., Sambrook, J. F., Gething, M. J., and Mitchell, C. A. (2001) *J. Biol. Chem.* **276,** 7643–7653
29. Resh, M. D. (1994) *Cell* **76,** 411–413
30. Field, K. A., Holowka, D., and Baird, B. (1995) *Proc. Natl. Acad. Sci. U. S. A.* **92,** 9201–9205
31. Rodgers, W. (2002) *BioTechniques* **32,** 1044–1051
32. Jordan, S., and Rodgers, W. (2003) *J. Immunol.* **171,** 78–87
33. Pettitt, T. R., Dove, S. K., Lubben, A., Calaminus, S. D., and Wakelam, M. J. (2006) *J. Lipid Res.* **47,** 1588–1596
34. Rodgers, W., and Zavzavadjian, J. (2001) *Exp. Cell Res.* **267,** 173–183
35. Penninger, J. M., and Crabtree, G. R. (1999) *Cell* **96,** 9–12
36. Acuto, O., and Cantrell, D. (2000) *Annu. Rev. Immunol.* **18,** 165–184
37. Villalba, M., Bi, K., Rodriguez, F., Tanaka, Y., Schoenberger, S., and Altman, A. (2001) *J. Cell Biol.* **155,** 331–338
38. Charras, G. T., Hu, C. K., Coughlin, M., and Mitchison, T. J. (2006) *J. Cell Biol.* **175,** 477–490
39. Caroni, P. (2001) *EMBO J.* **20,** 4332–4336
40. Roelants, G., Forni, L., and Pernis, B. (1973) *J. Exp. Med.* **137,** 1060–1077
41. Gabev, E., Kasianowicz, J., Abbott, T., and McLaughlin, S. (1989) *Biochim. Biophys. Acta* **979,** 105–112
42. Shan, X., Czar, M. J., Bunnell, S. C., Liu, P., Liu, Y., Schwartzberg, P. L., and

Wange, R. L. (2000) *Mol. Cell. Biol.* **20,** 6945–6957
43. Arrieumerlou, C., Randriamampita, C., Bismuth, G., and Trautmann, A. (2000) *J. Immunol.* **165,** 3182–3189
44. Jaffe, A. B., and Hall, A. (2005) *Annu. Rev. Cell Dev. Biol.* **21,** 247–269
45. Zhang, W., Sloan-Lancaster, J., Kitchen, J., Trible, R. P., and Samelson, L. E. (1998) *Cell* **92,** 83–92
46. Zhang, W., Irvin, B. J., Trible, R. P., Abraham, R. T., and Samelson, L. E. (1999) *Int. Immunol.* **11,** 943–950
47. Zhang, W., Trible, R. P., and Samelson, L. E. (1998) *Immunity* **9,** 239–246
48. Zhu, M., Shen, S., Liu, Y., Granillo, O., and Zhang, W. (2005) *J. Immunol.* **174,** 31–35
49. Wang, J., Arbuzova, A., Hangyas-Mihalyne, G., and McLaughlin, S. (2001) *J. Biol. Chem.* **276,** 5012–5019
50. Tong, J., Nguyen, L., Vidal, A., Simon, S. A., Skene, J. H., and McIntosh, T. J. (2008) *Biophys. J.* **94,** 125–133
51. van Rheenen, J., Achame, E. M., Janssen, H., Calafat, J., and Jalink, K. (2005) *EMBO J.* **24,** 1664–1673
52. Stauffer, T. P., Ahn, S., and Meyer, T. (1998) *Curr. Biol.* **8,** 343–346
53. Varnai, P., and Balla, T. (1998) *J. Cell Biol.* **143,** 501–510
54. Lemmon, M. A., and Ferguson, K. M. (2001) *Biochem. Soc. Trans.* **29,** 377–384
55. Varnai, P., Lin, X., Lee, S. B., Tuymetova, G., Bondeva, T., Spat, A., Rhee, S. G., Hajnoczky, G., and Balla, T. (2002) *J. Biol. Chem.* **277,** 27412–27422